Glacial Earthquakes in Greenland and Antarctica

Meredith Nettles and Göran Ekström

Lamont-Doherty Earth Observatory of Columbia University, Palisades, New York 10964;
email: nettles@ldeo.columbia.edu

Key Words

glacier, calving, seismicity, climate change, geodesy

Abstract

Glacial earthquakes are a new class of seismic events, first discovered as
signals in long-period seismograms recorded on the Global Seismographic
Network. Most of these events occur along the coasts of Greenland, where
they are spatially related to large outlet glaciers. Glacial earthquakes show a
strong seasonality, with most events occurring during the late summer. The
rate of glacial-earthquake occurrence increased between 2000 and 2005, with
a stabilization of earthquake frequency at 2003–2004 levels in 2006–2008.
Recent observations establish a strong temporal correlation between the dis-
tinct seismic signals of glacial earthquakes and large ice-loss events in which
icebergs of cubic-kilometer scale collapse against the calving face, linking
the seismogenic process to the force exerted by these icebergs on the glacier
and the underlying solid earth. A sudden change in glacier speed results from
these glacial-earthquake calving events. Seasonal and interannual variations
in glacier-terminus position account for general characteristics of the tem-
poral variation in earthquake occurrence. Glacial earthquakes in Antarctica
are less well studied, but they exhibit several characteristics similar to glacial
earthquakes in Greenland.

1. INTRODUCTION

The term glacial earthquake refers to a class of seismic events that occurs in geographical association with moving glaciers. Glacial earthquakes generate large-amplitude, long-period seismic waves that are recorded all over the world, but because the signals from these earthquakes differ from those of regular earthquakes, standard methods of earthquake monitoring cannot be used to detect or locate them. Their existence was therefore not known until 2003, when the application of a new method of earthquake detection revealed the occurrence of dozens of earthquakes with distinct characteristics in glaciated areas of Greenland, Antarctica, and Alaska (Ekström et al. 2003). Increasing numbers of glacial earthquakes were detected in Greenland in the years 2000–2005 (Ekström et al. 2006), suggesting a link between the earthquakes and the accelerating mass loss and melting of the Greenland ice sheet.

A wide range of seismic phenomena are observed in glacial environments as a result of processes such as the stick-slip sliding, cracking, and falling of ice (e.g., Weaver & Malone 1979, Wolf & Davies 1986, Qamar 1988, Anandakrishnan & Bentley 1993, Deichmann et al. 2000, Stuart et al. 2005, O'Neel et al. 2007, Walter et al. 2008, Jónsdóttir et al. 2009). All studies of glacier seismicity before the study of Ekström et al. (2003), however, describe small-magnitude earthquakes ($M <$ 3.0) generating primarily high-frequency seismic energy. In contrast, glacial earthquakes have magnitudes of $M \sim 5$ and emit long-period ($T > 30$ s) seismic waves. These distinct characteristics motivated the use of a specific label to describe this new class of earthquake.

The initial evidence for glacial earthquakes was entirely seismological, consisting of seismic signals recorded at hundreds to thousands of kilometers from the events. Early conjectures for the physical mechanism of glacial earthquakes, based on the detailed analysis and interpretation of the seismological data, led to the hypothesis that the earthquakes were generated by the sudden sliding motion of a large volume of glacier ice. This hypothesis, and competing ones, were tested starting in the summer of 2006 with field deployments of Global Positioning System (GPS) receivers and other geophysical instrumentation at earthquake-generating outlet glaciers in Greenland. Results from these investigations show a clear spatial and temporal correlation between glacial earthquakes and major calving events, with large-scale, sudden mass displacements limited to the calving ice volume. Recent observations also indicate that the glacial earthquakes and calving events cause abrupt and persistent changes in glacier velocity.

Glacial earthquakes are one of several phenomena associated with rapid changes in the dynamics of ice sheets and glaciers that have received increasing attention in the context of a changing climate. In this article, we first review the discovery of glacial earthquakes as a seismological phenomenon and discuss their seismological characteristics. We present earthquake-detection results for Greenland and Antarctica updated through 2008 and review the evolving understanding of glacial earthquakes that has resulted from several investigations of rapidly moving outlet glaciers in Greenland. We summarize the observations available for Antarctica. Finally, we present a number of questions that remain unanswered regarding the nature of glacial earthquakes and the related dynamics of the large outlet glaciers where they occur.

2. GLACIAL EARTHQUAKES IN GREENLAND

Most studies of glacial earthquakes since the 2003 report by Ekström et al. have focused on earthquakes in Greenland. In this section, we review the seismological constraints on the glacial-earthquake source process and early interpretation of the physical mechanism for these unusual events. We provide updated detection results through 2008 and discuss these results in the context of observations and discoveries since 2006.

2.1. Initial Detection and Explanation

Greenland's glacial earthquakes eluded earlier discovery because they possess source characteristics different from those of standard tectonic earthquakes. Tectonic earthquakes, which result from the release of elastic stress across a fault surface, have durations that increase with the magnitude of the earthquake. Typically, a $M = 5$ earthquake has a duration of ~ 2 s and a $M = 7$ earthquake has a duration of ~ 20 s. The amplitude spectrum of the elastic waves radiated by an earthquake depends on the duration of the source. At periods longer than the source duration, the spectrum is relatively flat; at shorter periods the spectrum falls off rapidly. For an earthquake of a given size, a longer source duration results in the relative depletion of radiated high-frequency energy. Standard methods of earthquake monitoring (detection and location) depend on the identification of high-frequency (1-s) P waves in seismograms. Moderate-size earthquakes with long durations radiate little high-frequency energy and may therefore elude detection because these low-amplitude, high-frequency signals can be buried in the earth's noise.

The largest glacial earthquakes in Greenland generate long-period ($T > 30$ s) seismograms that are similar in amplitude to those generated by a moment-magnitude $M_W = 5$ tectonic earthquake. **Figure 1** shows the globally recorded long-period signals from one Greenland event, illustrating the large amplitude of the seismic signals even at long distances. None of the Greenland events appears, however, in standard earthquake catalogs. These catalogs rely on the detection of high-frequency radiation, and the omission of the glacial earthquakes is consistent with a slow source process and depletion of high-frequency energy. The detection of glacial earthquakes followed the development and application of a new algorithm designed to identify seismic sources globally on the basis of their generation of long-period seismic waves (Ekström & Nettles 2002, Ekström 2006). The algorithm is based on array-processing techniques. Vertical-component seismograms from the global network of seismic stations are filtered between 35 and 150 s and phase adjusted to correct for Rayleigh wave propagation delays from a test location to each station. When the location corresponding to a seismic event is found, all the signals will be in phase. **Figure 1** shows an example of the alignment of the corrected Rayleigh wave arrivals for one of the detected earthquakes in Greenland.

The initial systematic application of the detection algorithm to three years of data (1999–2001) from the Global Seismographic Network (GSN) led to the identification of 46 previously unreported earthquakes of $4.6 \leq M \leq 5.0$ in glaciated areas of Greenland, Alaska, and Antarctica, with 42 of the events located along the eastern and western coasts of Greenland (Ekström et al. 2003). In addition to their slow character, these earthquakes were shown to generate seismic surface waves that were not well explained by the standard moment-tensor representation of stress release used for tectonic earthquakes. The surface waves were found instead to be well fit by a single-force source model (Kawakatsu 1989), which describes the forces acting on the solid earth during a landslide. In this source model, a force acts on the earth in the direction opposite the acceleration of the sliding mass. For a mass accelerating down an incline, the force acts in the updip direction, opposite the direction of sliding. When the mass decelerates, the force acts in the downdip direction. Modeling the seismograms through the use of this approach yields estimates of the sliding direction as well as the product of sliding mass and total sliding distance. In the 2003 study, investigation of five of the best-recorded Greenland earthquakes yielded force directions consistent with gravitational sliding toward the coast. For a glacial earthquake of $M = 5$, the corresponding mass-distance product is approximately 10^{14} kg m, and the 2003 study hypothesized that the glacial-earthquake phenomenon involved a large mass of ice (e.g., 10^{13} kg, or ~ 10 km^3) sliding a relatively short distance (e.g., 10 m).

Further characteristics of Greenland's glacial earthquakes were revealed in an analysis of global seismic data from 1993 through 2005 (Ekström et al. 2006). The analysis resulted in 182 earthquake
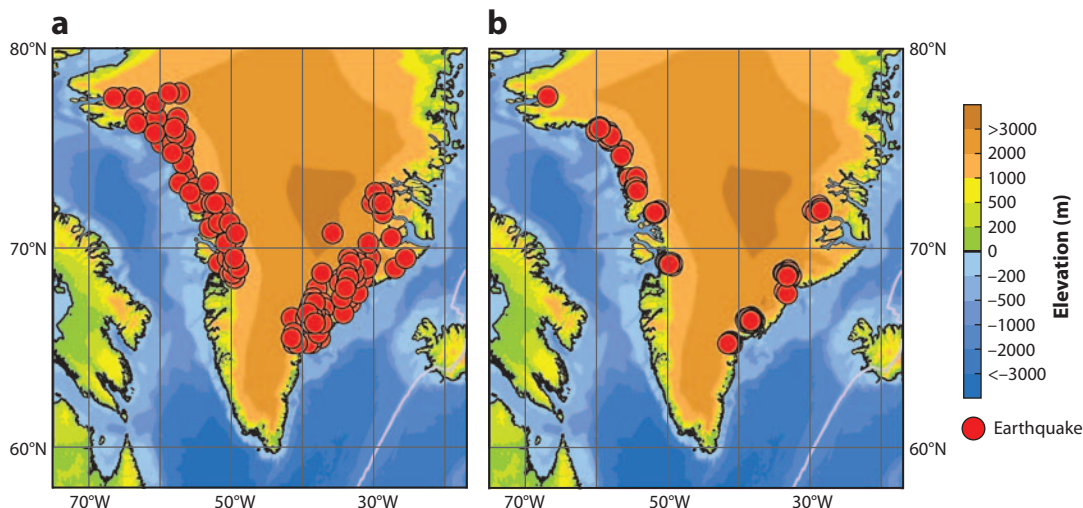
GSN: Global Seismographic Network
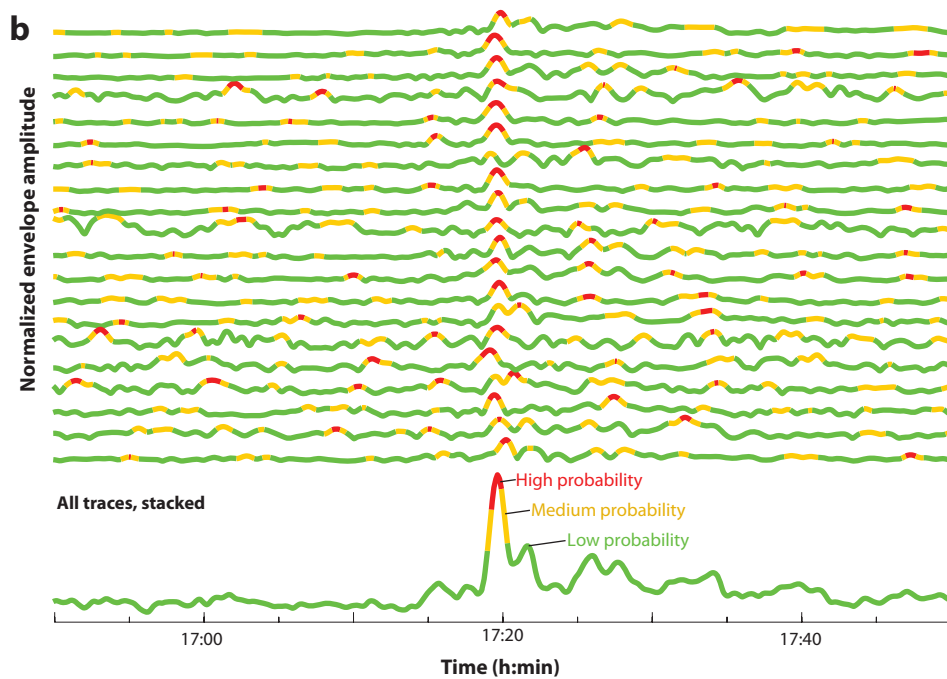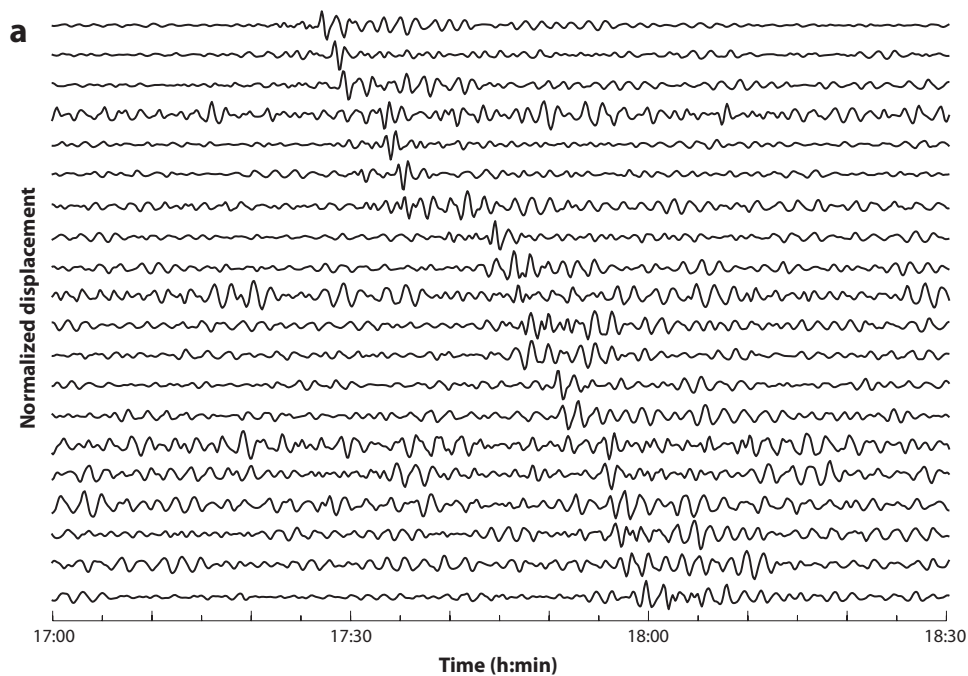
Figure 2

(*a*) Map showing 252 glacial earthquakes in Greenland for the period 1993–2008, detected and located using the surface-wave detection algorithm. (*b*) Map showing the improved locations of 184 glacial earthquakes for the period 1993–2005 analyzed in detail by Tsai & Ekström (2007). Note the tight clustering of the relocated earthquake epicenters near major outlet glaciers.

detections along the coast of Greenland (**Figure 2**). All events were found to be spatially correlated with major outlet glaciers of the Greenland ice sheet. Glacial earthquakes were also found to be a strongly seasonal phenomenon, with most earthquakes occurring in July and August and few occurring in January and February (**Figure 3**). Most dramatically, the 2006 study found a clear increase in the number of glacial earthquakes occurring in Greenland: An average of 10 events per year occurred in the period 1993–2000, rising to 21 events in 2003, 27 in 2004, and 33 in 2005 (**Figure 3**).

Tsai & Ekström (2007) modeled seismograms from all the 1993–2005 Greenland earthquakes by using the landslide model of the earthquake source process to obtain improved locations for the glacial earthquakes as well as quantitative estimates of the earthquake source parameters. As shown in **Figure 2**, the improved locations are tightly clustered near a number of Greenland's large outlet glaciers. Tsai & Ekström (2007) found that force directions in the events were consistent with sliding in the direction of glacier flow, and that typical source durations were ∼50 s. The analysis led to estimates of the product (mass × sliding distance) in the range of 0.1 to 2.0 × 10^{14} kg m, and the authors noted that the distribution of earthquake sizes was different at different outlet glaciers. In particular, the size distribution for events at Kangerdlugssuaq glacier is peaked above

Figure 1

(*a*) Long-period Rayleigh wave arrivals at globally distributed stations ranging in distance from 19° (*top trace*) to 154° for a glacial earthquake at Kangerdlugssuaq glacier, East Greenland, on December 28, 2001. (*b*) Seismograms after propagation effects from the source location to each station have been removed, and the envelope of the waveform has been calculated. The coloring of each seismogram reflects the probability that surface-wave energy has been detected; red indicates the highest probability. The bottom trace is a stack of the individual station traces. The alignment of the individual detections indicates the presence of Rayleigh wave energy emanating from a location near Kangerdlugssuaq glacier.
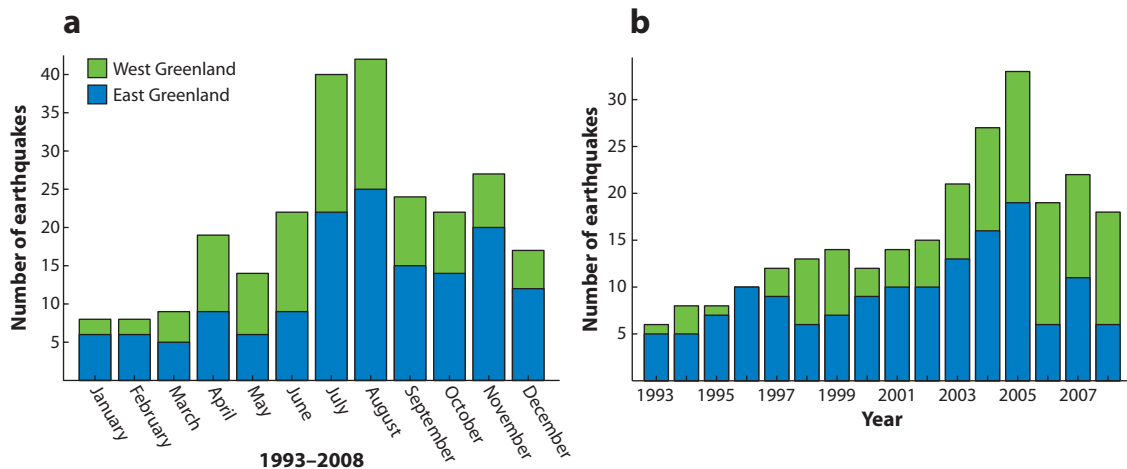
Figure 3

(*a*) Histogram showing seasonality of glacial earthquakes in Greenland based on detections for 1993–2008. Bars show the number of earthquakes per month detected in Greenland. (*b*) Histogram showing the number of glacial earthquakes detected in Greenland each year since 1993.

the detection threshold of $M = 4.6$, suggesting the existence of a characteristic earthquake size at that glacier.

2.2. Recent Detections

We have extended the detection time series of glacial earthquakes in Greenland for the period 2006–2008 using the same algorithm, data sources, and detection criteria as in the earlier studies (Ekström et al. 2003, 2006). In earlier tabulations of events, we have followed Ekström (2006) and excluded C-quality detections that coincided in time with another global detection; we refer to these events as E-quality detections. After inspecting these detections individually (14 for the period 1993–2008) and confirming that they correspond to real seismic sources, we have included them in the results shown here and the discussions that follow. Fifty-nine earthquakes were detected during 2006–2008; source parameters for these events are listed in **Table 1**, and **Figure 2** shows all glacial-earthquake detections in Greenland for the period 1993–2008. (The full list of events for 1993–2008, as well as recent updates, is available at **http://www.globalcmt.org**.) The trend of increasing earthquake numbers observed through 2005 has not continued in the period 2006–2008, although activity during the past few years remains higher than in the 1990s, at levels similar to 2003–2004. Western Greenland currently generates large numbers of glacial earthquakes: Eleven or more earthquakes have been detected in each of the five most recent years, compared with an average of 4.5 events per year for the same region during the period 1993–2003.

2.3. Current Understanding of Events in Greenland

The results described in the previous section have motivated a number of focused studies aimed at obtaining a better understanding of the glacial-earthquake source mechanism and the relation of the earthquakes to glacier dynamical processes. Satellite remote-sensing studies (Joughin et al. 2008a), field-based observational campaigns (Amundson et al. 2008, Nettles et al. 2008a,

Table 1 Source parameters for 59 glacial earthquakes in Greenland[a]

Date	Time	Latitude	Longitude	M	Date	Time	Latitude	Longitude	M
2006/02/13	20:29:52	70.25	−30.75	4.8C	2007/08/03	19:25:12	72.25	−52.25	4.8C
2006/02/28	22:44:32	69.00	−33.00	4.8A	2007/08/13	20:37:52	66.25	−38.75	4.8B
2006/03/04	23:05:20	65.75	−41.25	4.7B	2007/08/25	09:19:04	75.25	−56.75	4.9A
2006/04/29	11:39:12	65.25	−41.25	4.8B	2007/09/11	22:42:00	70.25	−50.75	4.6C
2006/05/01	06:44:32	72.25	−52.75	4.9A	2007/10/13	05:55:12	74.75	−56.75	4.8A
2006/06/24	10:48:32	69.25	−49.75	4.7E	2007/11/21	18:04:56	66.25	−38.75	5.0A
2006/07/10	18:13:36	65.25	−40.75	4.8A	2007/11/24	00:08:56	68.50	−33.50	4.8A
2006/07/16	03:15:28	69.00	−31.00	4.6C	2007/11/24	12:54:32	66.50	−38.50	4.9A
2006/07/16	06:41:52	73.25	−53.25	4.7C	2007/11/24	13:29:52	67.25	−38.25	4.8A
2006/07/25	04:51:44	68.75	−49.75	4.7C	2007/12/14	06:39:36	75.25	−56.75	4.9A
2006/08/10	18:45:20	77.50	−65.50	4.8B	2007/12/31	14:40:56	66.25	−38.75	4.9A
2006/08/23	17:19:28	65.75	−37.75	4.7C	2008/02/14	05:12:24	72.75	−55.75	4.8B
2006/08/28	07:55:04	69.50	−25.50	4.6B	2008/04/05	21:06:08	75.50	−56.50	4.8A
2006/09/10	04:20:16	77.75	−57.25	4.9C	2008/04/07	13:58:00	74.25	−56.75	4.7C
2006/10/09	04:03:12	76.50	−60.50	4.8B	2008/05/04	12:52:40	65.50	−41.50	4.8B
2006/10/14	07:23:20	76.00	−58.00	4.8B	2008/05/28	21:06:40	70.75	−49.25	4.7B
2006/11/05	09:13:04	75.75	−58.25	4.7C	2008/06/12	17:20:08	69.00	−49.00	4.7E
2006/11/28	10:55:44	68.75	−32.75	4.9B	2008/06/13	15:40:40	75.75	−57.75	4.8C
2006/12/19	16:57:44	74.75	−57.75	4.8B	2008/06/19	15:20:00	74.75	−58.25	4.8B
2007/04/22	08:55:04	66.25	−38.25	4.7A	2008/07/13	04:59:44	69.50	−49.50	4.8C
2007/04/23	21:56:56	75.25	−58.25	4.8A	2008/08/01	14:43:20	66.50	−38.50	4.8A
2007/05/30	02:57:12	77.50	−63.50	4.7C	2008/08/01	23:00:40	66.75	−39.25	4.8A
2007/06/09	05:16:56	75.75	−60.75	4.8B	2008/08/14	20:58:24	77.75	−58.75	5.0A
2007/07/04	16:55:20	69.25	−49.75	4.9A	2008/08/19	21:05:28	66.25	−38.25	4.8B
2007/07/09	01:08:16	66.25	−37.25	4.8A	2008/11/03	16:44:48	68.75	−33.75	4.9B
2007/07/09	02:42:08	66.75	−38.25	4.7B	2008/11/07	13:44:24	77.50	−66.50	4.7E
2007/07/09	05:31:12	75.00	−57.00	4.6C	2008/11/21	20:31:52	76.00	−58.00	4.9A
2007/07/20	00:36:16	69.25	−33.25	4.7A	2008/11/25	04:10:40	68.50	−33.50	4.9A
2007/07/24	23:03:12	77.25	−60.75	4.9A	2008/12/13	14:47:52	68.00	−34.00	5.0A
2007/07/26	22:42:48	66.50	−38.50	4.7A					

[a]Origin times and epicenters for 59 glacial earthquakes in Greenland, 2006–2008. The letter code following the magnitude M indicates the quality of the detection and location: A is the highest quality and C/E is the lowest. Magnitudes are calibrated as described by Ekström (2006).

Rial et al. 2009), and theoretical studies (Tsai et al. 2008) have been undertaken with primary goals of identifying the physical process that generates the teleseismically observed seismic waves and understanding the earthquakes' seasonality and increasing frequency. Great progress in answering these questions has been achieved during the several years since the initial identification of the earthquakes by Ekström et al. (2003). In particular, glacial-earthquake occurrence has been clearly and convincingly linked to major calving events at the glacier front.

2.3.1. The earthquake source mechanism. In 2006, we initiated, together with colleagues in the United States, Denmark, and Spain, a geodetic field study at Helheim glacier, East Greenland, aimed at measuring glacier deformation associated with the glacial earthquakes occurring there.
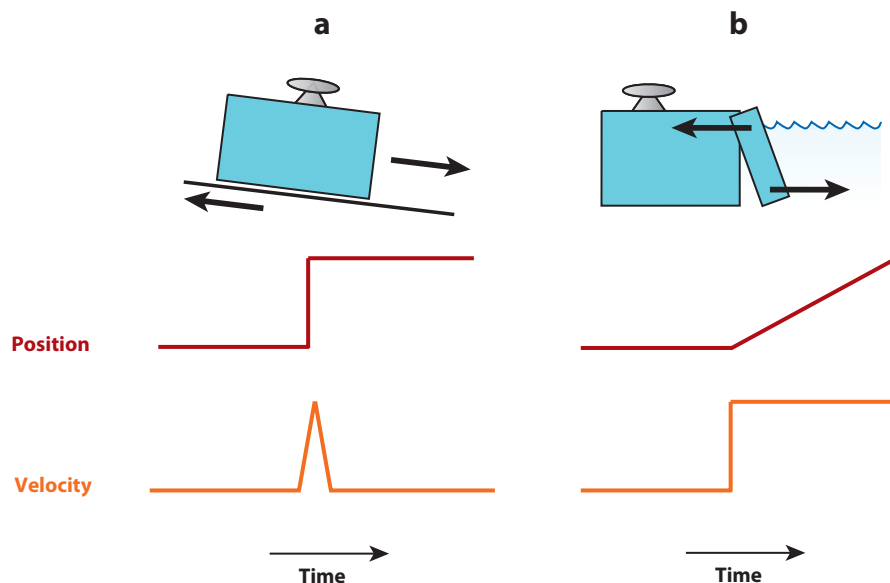
Figure 4

Schematic showing position and velocity expected on the surface of a glacier, at a location shown by the disk-shaped GPS antenna, for a glacial earthquake source model in which (*a*) the trunk of the glacier lurches forward abruptly, as suggested by Ekström et al. (2003), and (*b*) resistance to flow in the glacier trunk is reduced as a result of a large calving event. The position curves are drawn as residuals with respect to an assumed-constant preearthquake velocity.

One goal was to validate or falsify the prediction of glacier motion implied by the hypothesis of Ekström et al. (2003) that the glacial earthquakes involved the sudden displacement of a large volume of the glacier trunk. This prediction is shown schematically in **Figure 4**. Helheim glacier is one of the largest outlet glaciers in Greenland and has produced approximately a quarter of the glacial earthquakes observed in Greenland to date. In this study, Nettles et al. (2008a) installed GPS receivers on the surface of the glacier (**Figure 5**) and at several stable, rock-based reference points nearby to allow for high-accuracy, high-time-resolution measurements of glacier motion before, during, and after glacial earthquakes. Several types of auxiliary geophysical data were also collected at and near Helheim glacier, including water-pressure data in the Helheim fjord system. The GSN was monitored using the techniques of Ekström et al. (2003, 2006) and Ekström (2006) to identify glacial earthquakes. A similar network has been operated by the same group of collaborators during each of the following summers.

Although no glacial earthquakes were initially found to have occurred at Helheim during the period of network operation in 2006 (one event has since been identified through analysis of a more complete GSN data set), several earthquakes occurred during the GPS network operation period in 2007 and 2008; data from the 2009 experiment are currently undergoing analysis. As reported by Nettles et al. (2008a), a joint analysis of the GPS and seismic data from 2007 produced an unexpected result: No step in displacement of the glacier surface occurs at the time of a glacial earthquake; instead, a distinct increase in velocity is observed (**Figure 6**). The increase in velocity occurs along the length of the glacier, from the calving front to a distance of at least 20 km upstream (**Figure 6**). The amplitude of the velocity change decreases with increasing distance from the calving front. For the event shown in **Figure 6**, velocity increases near the calving front
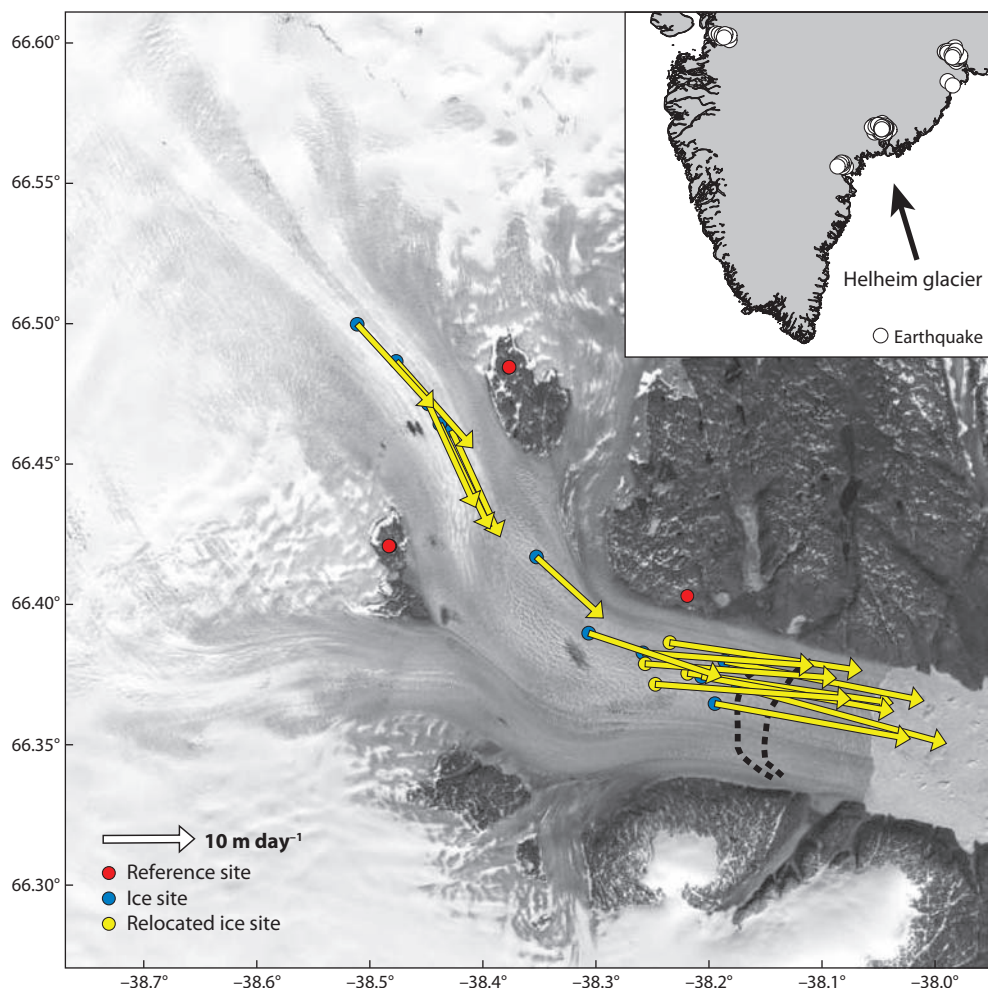
Figure 5

Map showing locations of GPS stations (*blue and yellow dots*) operated by Nettles et al. (2008a) on Helheim glacier during July and August 2007, overlain on a 2001 Landsat image. Arrows show average velocities over this time period. The GPS stations nearest the calving front were moved mid-season to the locations shown by the yellow dots. Red dots represent locations of rock-based GPS reference sites. Dashed lines show the location of the calving front at the beginning (*eastern line*) and end (*western line*) of the network operation period. Inset shows location of Helheim glacier in southeast Greenland (*black arrow*) and locations of glacial earthquakes (*white dots*) after Tsai & Ekström (2007).

are nearly 6% (1.3 m day^{-1}). However, these velocity increases, even if assumed to occur on the observed timescale of the earthquakes (30–60 s) and to involve the mass of the entire glacier trunk, would produce a force too small to explain the seismic radiation observed globally. The glacier acceleration thus cannot represent the earthquake source.

Analysis of satellite imagery and water-pressure data collected near Helheim glacier shows, however, that large calving events also occur at the times of the glacial earthquakes. The collapse of a large ice mass into the glacial fjord generates a small tsunami; the tsunami arrival times constrain the timing of the ice-loss events to within a few minutes. Mapping of calving-front locations using Moderate Resolution Imaging Spectroradiometer (MODIS) imagery confirms the loss of an area

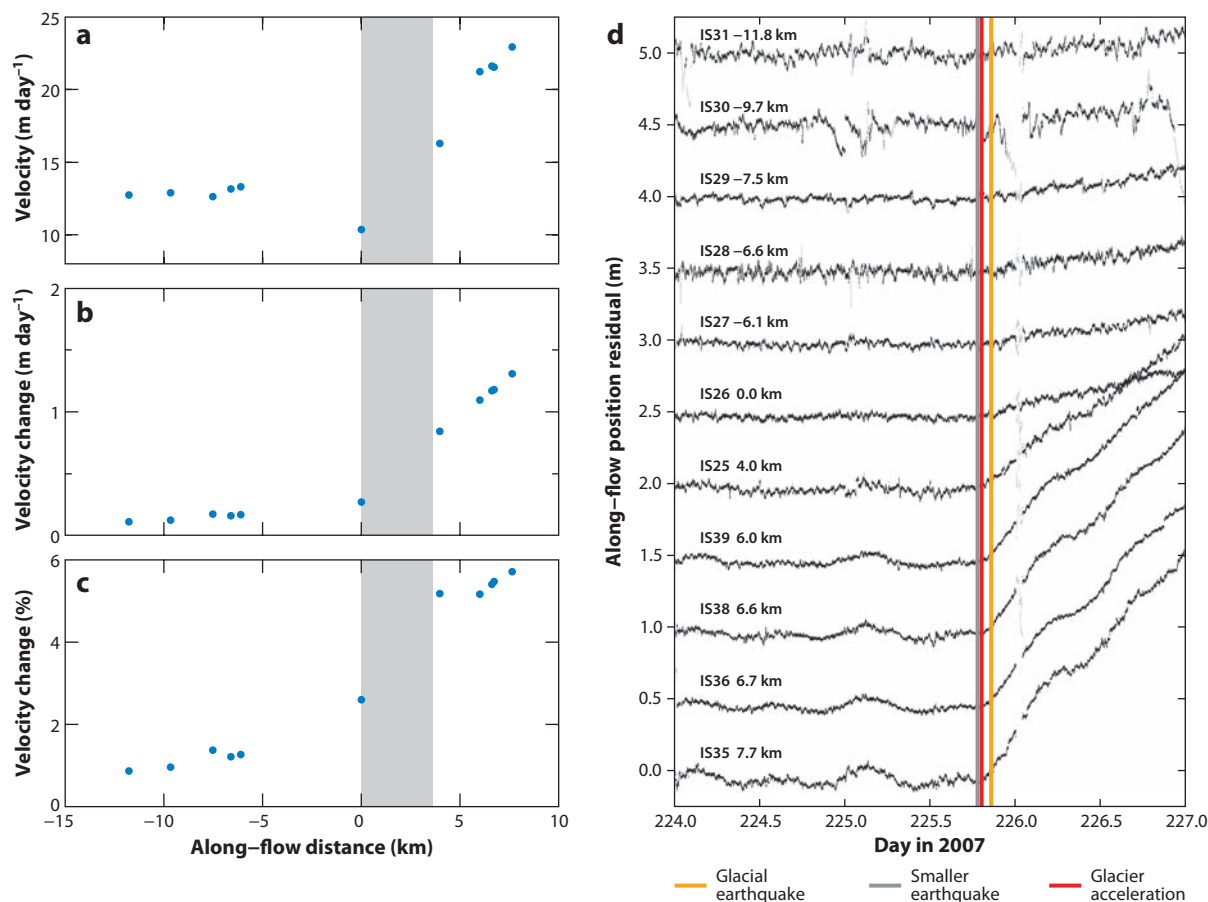**MODIS:** Moderate Resolution Imaging Spectroradiometer

Figure 6

Change in glacier velocity at the time of a glacial earthquake at Helheim glacier on August 13 (day of year 225), 2007, after Nettles et al. (2008a). (*a*) Preearthquake glacier velocity and (*b*) absolute and (*c*) relative changes in glacier speed with distance along the glacier. The distance scale is positive in the glacier-flow direction. Gray region shows the area corresponding to the bend in the glacier (**Figure 5**). (*d*) Along-flow displacement of GPS stations shown in **Figure 5**, plotted with respect to the preacceleration velocity at each station. Traces are offset for clarity and are ordered by distance along the glacier, with stations located nearest the calving front at the bottom of the plot. Each trace is labeled with the station name and distance along the flow line, as defined in panels *a–c*. Positions plotted in gray are outliers at the 4-σ level. Orange line shows the time of the glacial earthquake, detected as described in the text; gray line shows the time of a smaller earthquake identified by interactive examination of network waveforms (see Nettles et al. 2008a); red line shows time of glacier acceleration estimated independently from a fit to the GPS position estimates.

of ice at the calving front of approximately 2–6 km^2 at the times of the earthquakes, within a temporal resolution of 1–4 days.

The coincidence in time of large calving events and the glacial earthquakes, combined with the lack of coseismic displacement of the glacier trunk, implicates the calving events as the seismogenic source. The modeling of Ekström et al. (2003) and Tsai & Ekström (2007) shows that the seismic data are explained well by a landslide-type source with a mass-sliding product of amplitude 0.1–2 × 10^{14} kg m. In the studies of Ekström et al. (2003, 2006) and Tsai & Ekström (2007), this mass-sliding product was interpreted to result from a large mass—perhaps 10 km^3 of ice within the glacier trunk—sliding a relatively short distance of ∼1–10 m. Equally consistent with

the seismic modeling result is the acceleration of a smaller mass over a larger distance. A large, newly formed iceberg of approximately 0.5–1 km^3 accelerating away from the calving front must undergo a center-of-mass translation of only a few tens to a few hundred meters to produce a mass-sliding product like that observed. Consideration of the newly formed iceberg as the slide mass, and hence the seismogenic source, provides an explanation for the glacial earthquakes as part of the ice-loss process at the glacier calving front.

The observed acceleration of the glacier at the time of ice loss is consistent with the arguments of several authors (e.g., Dupont & Alley 2005, Howat et al. 2005, Nick et al. 2009) that iceberg calving can reduce resistance to flow sufficiently to cause significant glacier acceleration, a model shown schematically in **Figure 4**. In this interpretation, the loss of ice at the terminus leads to an increase in the effective driving stress applied to the glacier trunk. The amplitude of the velocity increase that results is controlled by the rheology of the ice, typically taken to exhibit power-law behavior with $n = 3$ (e.g., Paterson 1994).

The study of Nettles et al. (2008a) focused on earthquakes observed in 2007; the same coincidence in time of ice loss, glacial earthquakes, and abrupt glacier acceleration was also observed for earthquakes at Helheim in 2008 (Hamilton et al. 2008, Nettles et al. 2008b). Data from 2008 included first-person observations of large-scale ice collapse into the Helheim fjord at the time of one earthquake and time-lapse photographic recordings of several others, confirming the association between the earthquakes and the calving process.

Amundson et al. (2008), working at Greenland's largest outlet glacier, Jakobshavn Isbræ, independently reached similar conclusions regarding the link between iceberg calving, glacial earthquakes, and the glacier's response to these processes. These authors used time-lapse photographic observations, local high-frequency seismic recordings, tide-gauge data, and geodetic observations of glacier and iceberg motion to examine the glacier's response to large calving events. Of the calving events they report for the time period May 2007–May 2008, one event, on July 4, 2007, is associated with a teleseismically detected glacial earthquake (**Table 1**). For this event, Amundson et al. (2008) found an increase in along-flow speed for an optical-survey marker located approximately 1 km behind the calving front, but no step in displacement. They reported similar behavior at the times of other large calving events, which also generated large seismic signals at high frequency on their local seismograph but did not generate teleseismic detections of glacial earthquakes. For one such event, on May 21, 2007, data are available from several survey markers. At the time of calving, Amundson et al. (2008) observed an increase in velocity at four optical-survey markers located within several kilometers of the calving front, but again no step in displacement. The observed velocity increases are 0.5–1.5 m day^{-1} (~3%), of generally similar amplitude to those observed at Helheim during glacial earthquakes; as at Helheim, the acceleration amplitudes diminish with distance from the calving front, at least within this limited observation region. The May 21, 2007, event was not large enough to generate a glacial-earthquake detection, but our inspection of seismograms from the GSN shows that it did produce weak teleseismic signals at periods of 35–100 s.

A calving event on June 5, 2007, appears to show behavior similar to that on May 21, 2007, based on two optical-survey records, whereas another calving event on May 29, 2007, at Jakobshavn produced an increase in velocity approximately 1 km behind the calving front but not farther upglacier. The May 29 and June 5 events did not produce coherent seismic signals at teleseismic distances. It remains unclear whether calving events like those reported at Jakobshavn on May 29 and June 5, 2007, produce glacial earthquakes that simply lie below the teleseismic detection threshold or whether they are coupled differently to the solid earth as a result of geometry or other factors. That they generate a local, high-frequency signal is clear, and those signals resemble local seismic recordings made during calving at other glaciers, including Columbia glacier, Alaska

(O'Neel et al. 2007). Few broadband recordings at regional and short teleseismic distances are available for such events, however, so the character of the long-period ($T > 30$ s) seismic signal for events like these is not well known.

In contrast to observations at Helheim, in which velocity changes that result from glacial earthquakes are observed ∼20 km behind the glacier front (Nettles et al. 2008a), a GPS observation at this distance on Jakobshavn Isbræ shows no increase, and perhaps a decrease, in along-flow speed at approximately the time of the July 4, 2007, glacial earthquake (Amundson et al. 2008). It is thus possible that the upstream response of the two glaciers to large calving events differs. However, the key results of the Amundson et al. (2008) study, including the association between glacial earthquakes and large calving events along with the abrupt acceleration of the glacier at the time of the earthquakes, are in good agreement with those of Nettles et al. (2008a).

The results of the two focused field studies described here are also in good agreement with the systematic, multiyear remote-sensing study of Helheim and Kangerdlugssuaq glaciers carried out by Joughin et al. (2008a). These authors mapped the locations of the glacier calving fronts during the spring and summer seasons of 2001–2006, using 250-m resolution MODIS imagery, to generate a history of calving-front advance and retreat with a time resolution of a few days. Comparison with the record of glacial earthquakes (Ekström et al. 2006, Tsai & Ekström 2007) shows that glacial earthquakes at both glaciers occur at the times of large ice-loss events during all years examined (**Figure 7**). These ice-loss events, given the limited time resolution of the imagery data, may be composed of one or more large calving events, and occasionally two or more earthquakes are associated with a single imaged retreat of the calving front. Not all large-scale ice-loss events are associated with detected glacial earthquakes, however.

Studies at Greenland's three largest outlet glaciers thus provide a consistent view of the glacial-earthquake source. Similar studies in other glacial-earthquake source regions have not been conducted, but a striking feature of the glacial-earthquake locations, shown in **Figure 2**, is that all occur in association with large tidewater glaciers where calving events like those at Jakobshavn, Kangerdlugssuaq, and Helheim glaciers may be expected. The overall spatial distribution of earthquakes is also consistent with the marine-calving source mechanism. The earthquakes occur in the southeast, east, and northwest, where marine-terminating outlet glaciers are abundant. There are no known glacial earthquakes in the southwest, where the highest concentration of land-terminating glaciers is found (e.g., Moon & Joughin 2008), and no known earthquakes on the north or northeast coasts, where many glaciers drain into floating ice shelves.

Furthermore, the theoretical work of Tsai et al. (2008) demonstrates that calving processes at large outlet glaciers may be expected, at least under certain circumstances, to produce seismic signals with approximately the observed amplitudes and durations. In particular, Tsai et al. (2008) found that calving events involving acceleration of the calved ice mass, which they term nonequilibrium calving, could produce forces on the calving face, and hence the solid earth, that match seismological observations of the glacial earthquakes. A model in which the newly calved iceberg capsizes against the calving face was found to produce a force history of amplitude, duration, and direction similar to those observed. The match to observations of earthquake duration was improved by including effective-mass contributions from proglacial ice mélange like that commonly present in outlet-glacier fjords.

The need for newly calved icebergs to capsize in order to generate glacial earthquakes is supported anecdotally by the observation that no glacial earthquakes occurred during most of summer 2006 at Helheim glacier. During this period, most ice loss occurred in the form of large, tabular icebergs sufficiently wide to remain in an upright position as they moved away from the calving front. This difference in calving style, illustrated in **Figure 8**, was observed in the field (Nettles et al. 2006, 2008b) and in satellite imagery (Joughin et al. 2008a). It is hypothesized
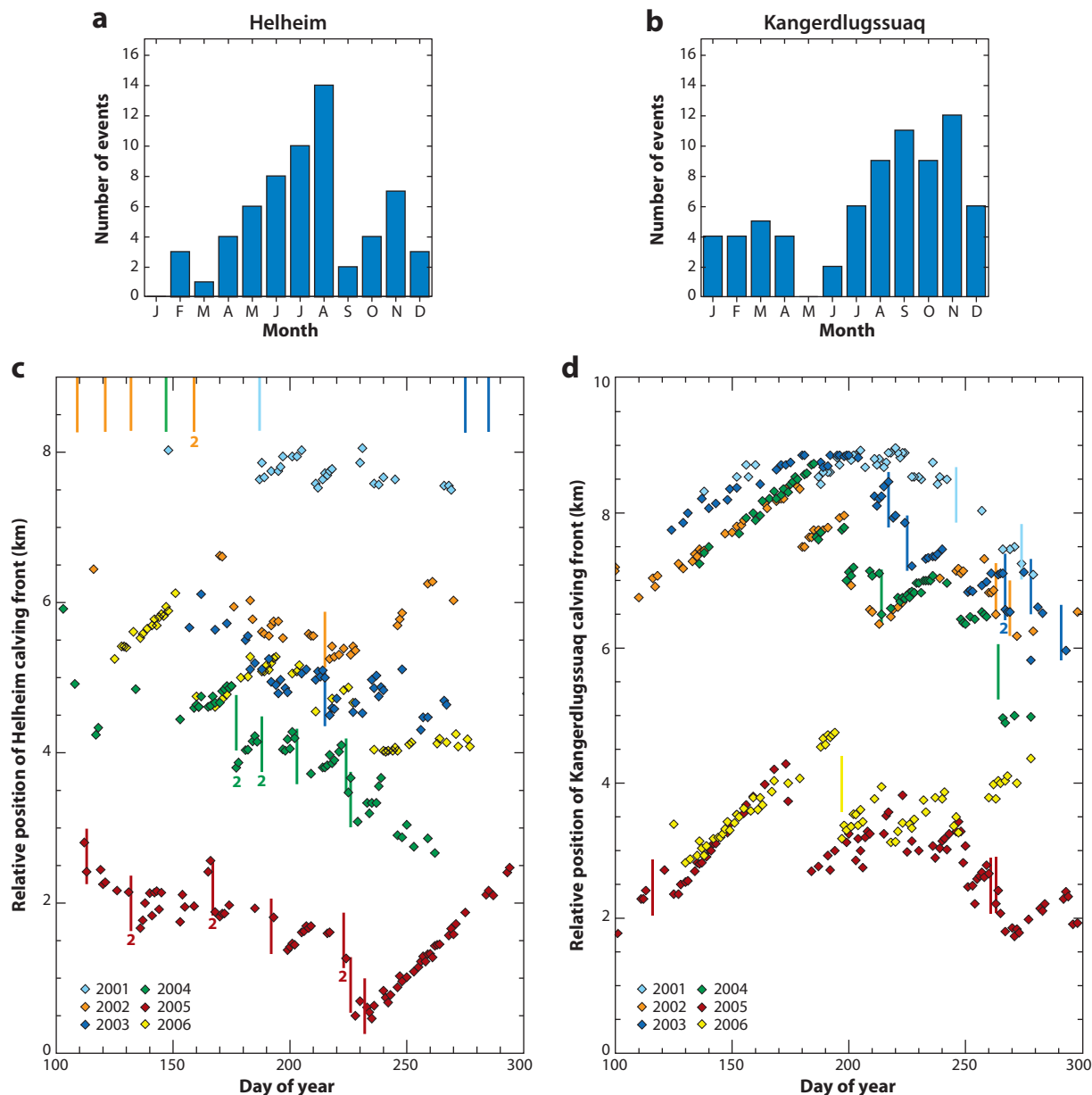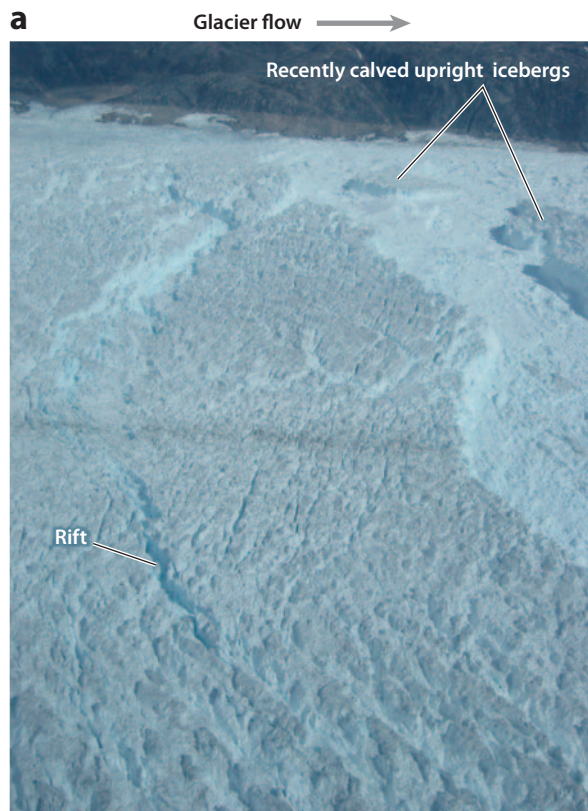
Figure 7

Seasonality of glacial earthquakes and calving-front position at Helheim and Kangerdlugssuaq glaciers. Number of glacial earthquakes occurring in each month during 1993–2008 is shown for (*a*) Helheim glacier and (*b*) Kangerdlugssuaq glacier. The relative position (*diamonds*) of the calving front is shown at (*c*) Helheim glacier and (*d*) Kangerdlugssuaq glacier, after Joughin et al. (2008a), based on analysis of MODIS imagery. Relative positions are positive in the glacier-flow direction. Short colored lines show the times of glacial earthquakes and are plotted at the top of the diagram when no calving-front position data are available. A number plotted by a line indicates multiple earthquakes on that day. Day of year (doy) 100 corresponds to April 10/11; doy 200, to July 19/20; and doy 300, to October 27/28.

a

Glacier flow →

Recently calved upright icebergs

Rift

b

← Glacier flow

70 m

⋯⋯ Horizontal iceberg
(700 m wide)

(Joughin et al. 2008a) that the difference in calving style is related to floatation conditions at the glacier terminus, with "silent" calving more likely to occur when a floating glacier tongue is present. Indeed, analysis of GPS time series recorded near the Helheim terminus during the summer of 2006 shows that the glacier had a short floating tongue (de Juan et al. 2008).

2.3.2. Earthquake size. Glacial earthquakes exhibit a magnitude-frequency distribution distinctly different from that of tectonic earthquakes. Globally, and in most tectonic regions, the magnitude-frequency relationship has a slope such that, during a given time period, 10 times fewer earthquakes occur for each unit increase in magnitude. Glacial-earthquake data are available for the period 1993–2008, a time period during which 252 earthquakes of $M \sim 4.6$–5.1 were observed in Greenland. The magnitude-frequency relation for tectonic earthquakes suggests that we should have observed ~ 25 earthquakes one magnitude unit larger, $M \sim 5.6$–6.1, during the same time period. The maximum observed magnitude for a glacial earthquake in Greenland is, however, $M = 5.1$, suggesting a low upper limit on glacial-earthquake size.

Knowledge of the smaller-magnitude end of the magnitude-frequency relation is limited by our ability to detect glacial earthquakes of magnitudes smaller than approximately $M \sim 4.6$. Observations of the glacial-earthquake size distribution at Helheim and Kangerdlugssuaq glaciers (Tsai & Ekström 2007), the two glaciers producing the largest numbers of glacial earthquakes, show some evidence for a preferred or characteristic earthquake size at different glaciers, however. The distribution of event size at Kangerdlugssuaq shows a peak at a mass-sliding product of 0.6×10^{14} kg m, whereas the event-size distribution at Helheim peaks at a value half as large.

The interpretation of the glacial-earthquake source in terms of the force exerted on the calving face by a capsizing iceberg provides at least a partial explanation of the upper limit on glacial-earthquake size and of differences in earthquake size between glaciers. For an iceberg to capsize, it must generally be narrower in the along-flow direction than it is high. The maximum iceberg height is controlled by the glacier thickness, and the thickness of the glacier thus also represents the maximum width of an iceberg that may capsize. The thickness of the glacier (maximum iceberg height) will also limit the lateral translation of the center of mass that occurs while the capsizing iceberg is in contact with the calving face. The cross-flow dimension of calved icebergs can be no larger than the glacier width, and is typically smaller.

The cross-flow width and the thickness of the glacier thus limit the maximum size of an earthquake that may be produced at a given glacier, and these physical characteristics of the glacier near its terminus may combine to produce a characteristic range of earthquake sizes at each glacier. For an along-flow dimension of a capsizing iceberg that is a given fraction of the glacier thickness, a simple analysis demonstrates that an increase in glacier thickness (iceberg height) of only 25% is sufficient to increase the mass-sliding product by a factor of approximately two, because the thickness controls both along-flow width and the sliding distance. We therefore expect that the

←——

Figure 8

The calving front at Helheim glacier (see **Figure 5** for location), illustrating two different styles of calving. (*a*) On July 25, 2006, during a period without glacial earthquakes. The width of the ice to the right of the rift is approximately 1 km. Several large, recently calved icebergs that remained upright as they moved away from the calving front are visible at the top right of the photograph. View is to the north; glacier flow is to the right (east) in the image. (*b*) On August 19, 2008, during a large calving event that generated a glacial earthquake. View is to the south; glacier flow is to the left (east) in the images. Time progresses from the top image to the bottom, with the bottom image taken approximately 3 min after the top image. In the top photograph, the calving iceberg has begun to capsize, with the top of the iceberg rolling down to the right against the calving face. In the bottom photograph, the iceberg has reached a horizontal position, exposing its full thickness (~ 700 m). The height of the calving face is ~ 70 m.

glacier thickness is likely to provide the strongest control on the observed earthquake magnitudes. Although the bed topography of many Greenland glaciers is poorly known, variations in thickness of 25% between glaciers are reasonable: The thickness of Helheim glacier near its terminus is approximately 700 m (e.g., Joughin et al. 2008a), whereas the thickness of Jakobshavn Isbræ near its terminus is approximately 900 m (Clarke & Echelmeyer 1996, Amundson et al. 2008).

2.3.3. Seasonality. The link between large ice-loss events and the earthquakes also provides at least a partial explanation for the seasonal and temporal variations in earthquake frequency. Ekström et al. (2006) suggested meltwater-mediated control of the seasonal and temporal variations in earthquake occurrence, based on the observations that propagation of surface meltwater to the ice-sheet bed leads to acceleration of the ice sheet during the summer months (Zwally et al. 2002) and that the area of the ice sheet affected by surface melting has increased during recent years (e.g., Steffen et al. 2004). Increases in water pressure at the glacier bed were envisioned to reduce resistance to glacier sliding sufficiently to promote earthquake occurrence, as the trunk of the glacier lurched abruptly forward. The current understanding that glacial earthquakes are generated during the collapse of a large ice mass into the glacial fjord requires a new understanding of the cause for the observed seasonal and temporal variations in earthquake frequency.

The data collected by Joughin et al. (2008a) show that the position of the calving front varies seasonally at Helheim and Kangerdlugssuaq glaciers (**Figure 7**), advancing during the winter and early spring and retreating during the summer and fall. The calving terminus of Kangerdlugssuaq glacier typically continues its winter advance through early or mid-July, when it begins to retreat in a series of large-scale calving events. During each event, the front typically retreats by 1 km or more; satellite imagery shows that these retreats occur during a time period of less than one day. As noted above, these retreats are often associated with glacial earthquakes. Between ice-loss events, the calving front tends to readvance but does not recover its previous position before the next large calving event occurs. The result is a net retreat of the calving front during the summer and fall; at Kangerdlugssuaq, the retreat phase continues through at least October, after which no further high-time-resolution satellite data are available.

The behavior of the calving terminus at Helheim glacier is similar, but the retreat of the terminus starts earlier in the year, probably before mid-April, when the observations of Joughin et al. (2008a) begin each year. The end of the retreat season also appears to occur earlier at Helheim, with stabilization or readvance of the front position starting in late August or early September, although the time series at Helheim is not as complete as the time series at Kangerdlugssuaq.

The same general pattern of seasonal ice-front advance and retreat has been documented at Jakobshavn Isbræ by Joughin et al. (2008b). Joughin et al. (2008b) provide only monthly estimates of ice-front position (for the period September 2005–September 2007), so that the temporal pattern of advance and retreat cannot be compared in detail with that from Helheim and Kangerdlugssuaq, but the overall pattern is similar. The position of the calving front advances during the winter and retreats during the summer; the retreat begins in February or March, earlier than at Helheim or Kangerdlugssuaq, and the stabilization and readvance begins in July or August. That the summer retreat occurs in a series of discrete episodes, as at Helheim and Kangerdlugssuaq, is supported by the observations of Amundson et al. (2008).

The timing of seasonal advance and retreat of the calving front at these glaciers agrees with variations in the seasonal distribution of glacial-earthquake activity documented by Tsai & Ekström (2007) and shown in **Figure 7** for Helheim and Kangerdlugssuaq glaciers. Peak levels of glacial-earthquake activity are seen at Helheim in June–August, with peak activity at Kangerdlugssuaq occurring somewhat later, in September–November. Jakobshavn, which experiences comparatively few glacial earthquakes, shows a peak in June–July.

The wintertime advance and summertime retreat of the outlet glaciers are achieved by the reduction or shutdown in large-scale calving during the winter months, with an increase in calving during the summer months. The link between large-scale calving events and glacial earthquakes then explains the seasonal signal in earthquake occurrence at these glaciers.

2.3.4. Temporal variation.   The observations of calving-front and glacial-earthquake seasonality demonstrate that the earthquakes occur predominantly while the calving front is in a retreat phase. We might therefore expect that overall, yearly earthquake abundance would increase at glaciers experiencing a net interannual retreat of calving-front position.

Moon & Joughin (2008) studied changes in ice-front position at glaciers throughout Greenland during the period 1992–2007, approximately the same time period covered by the record of glacial-earthquake frequency shown in **Figure 3**. They analyzed satellite imagery to map calving-front positions at more than 200 of Greenland's largest glaciers, including those terminating in tidewater, during the periods 1992–2000, 2000–2006, and 2006–2007. In the earthquake record, the period 1993–2000 shows relatively steady but slightly increasing numbers of earthquakes from year to year. The years 2000–2005 show a dramatic increase in earthquake numbers, eventually reaching a level, in 2005, of approximately five times as many earthquakes as in 1993 and more than twice as many as in any year through 2000. The years 2006–2008 show lower levels of seismicity than in 2005, with earthquake frequency similar to that observed in 2003–2004. These variations in earthquake activity track overall ice-front activity in Greenland.

For 1992 to 2000, Moon & Joughin (2008) found small calving-front retreats at nearly all glaciers for which they were able to obtain measurements, with most glaciers showing retreat rates of 25–100 m year^{-1}. These glaciers are located along the northwest, east, and southeast coasts of Greenland, the same regions in which the earthquakes occur. In the period 2000–2006, they observed an increase in retreat rates relative to 1992–2000; nearly all glaciers they studied retreated, and many—including those in the particularly seismogenic regions of the southeast coast and the northeast Melville Bugt region—exhibited retreat rates greater than 200 m year^{-1}. Helheim, Kangerdlugssuaq, and Jakobshavn glaciers retreated at rates greater than 500 m year^{-1} during this time period (see also Joughin et al. 2004, Howat et al. 2005, Luckman et al. 2006, Howat et al. 2007, Stearns 2007). From 2006 to 2007, a cooler period, Moon & Joughin (2008) found reduced rates of retreat and some glacier-front advances in east and southeast Greenland. Northwest Greenland showed a mixed signal, with some glaciers showing stabilization or a small readvance but many showing continued retreat at rates of 25–500 m year^{-1}.

As can be seen in **Figure 3**, the increase in earthquake numbers between 2000 and 2005 was the result of increasing earthquake frequency in both East and West Greenland. In East Greenland, most of the increase was contributed by Helheim and the "Southeast Greenland" cluster [region 3 of Tsai & Ekström (2007)]. As retreat rates have decreased or reversed at these glaciers, earthquake occurrence rates in East Greenland have returned to approximately the preretreat levels of 1993–2000. In West Greenland, earthquake occurrence rates have remained at their high 2005 levels during 2006–2008, again showing good overall agreement between glacial-earthquake abundance and the pattern of glacier-front advance and retreat.

2.3.5. Summary of recent results for Greenland glacial earthquakes.   Recent results from field and remote-sensing studies and theoretical work provide a consistent picture of the glacial-earthquake source, illustrated schematically in the right side of **Figure 4**. Greenland's glacial earthquakes are coeval with, and causally linked to, large glacier-calving events. At the time of an earthquake, the glacier exhibits no coseismic offset in displacement, but rather an increase in velocity. The amplitude of the velocity increase associated with the earthquake is largest near the

calving front, diminishing with distance upglacier from the calving front. ==The long-period seismic signals observed globally appear to be produced as a newly formed, gravitationally unstable iceberg capsizes against the glacier calving face, transmitting the force associated with the acceleration of its center of mass away from the glacier to the calving face, and hence the solid earth.==

3. GLACIAL EARTHQUAKES IN OTHER REGIONS

The great majority of glacial earthquakes occur in Greenland, but small numbers of earthquakes with similar source characteristics have been detected in other glaciated areas. Ekström et al. (2003), for example, reported the detection of glacial earthquakes in Alaska and Antarctica. In addition to the glacial earthquakes detected using seismological techniques, other transient motions of glaciers have also been found to be associated with the emission of low-frequency seismic waves. In the following two subsections, we discuss the current understanding of glacial-earthquake detections in Antarctica and Alaska.

3.1. Glacial Earthquakes in Antarctica

For the period 1993–2008, the surface-wave detection analysis of seismograms from the GSN results in the identification of 14 new earthquakes in Antarctica. The events are listed in **Table 2** and shown in **Figure 9**. All the events are located near the edge of the ice sheet, with seven events clustered near Vincennes Bay, East Antarctica; three events on the coast of the Antarctic Peninsula; one event on the edge of the Filchner-Ronne Ice Shelf; one event on the Banzare Coast; and two events on the George V Coast. The geographical association of these 14 events with the edge of the Antarctic ice mass—and, in several cases, with major outlet glaciers of the Antarctic ice sheet—suggests that these earthquakes are analogous to those in Greenland and are likely to be associated with major calving events. The small number of detected events makes it difficult to draw inferences about seasonality or temporal variation of glacial-earthquake occurrence in Antarctica.

The small number of detected glacial earthquakes in Antarctica, as compared with Greenland, is likely to reflect a real scarcity of such events rather than a detection bias. An explanation for the difference may be tied to the mode of ice loss from the two ice sheets and to the more temperate conditions near Greenland. As described in Section 2.3.1, glacial earthquakes appear to require a calving style in which gravitationally metastable icebergs collapse against the calving face. The

Table 2   Source parameters for 14 detected earthquakes in Antarctica[a]

Date	Time	Latitude	Longitude	M	Date	Time	Latitude	Longitude	M
1996/07/14	19:05:52	−62.25	−55.75	4.8C	2002/03/30	04:15:28	−67.00	109.00	4.8C
1998/05/11	23:17:44	−67.00	109.00	4.9C	2004/01/24	08:38:24	−68.00	150.00	4.8C
1999/06/27	15:37:52	−77.75	−47.25	4.8C	2004/01/31	04:31:52	−67.00	111.00	4.9C
2000/04/09	23:25:36	−66.25	110.75	4.9B	2007/10/14	02:10:08	−66.75	109.75	4.9B
2000/06/22	23:10:48	−67.00	109.00	4.9C	2008/05/18	08:35:04	−65.50	124.50	4.8C
2001/11/24	03:20:48	−67.00	109.00	4.9E	2008/06/18	00:04:00	−68.75	151.25	4.8B
2002/03/18	08:22:40	−65.25	−62.75	4.7C	2008/07/21	07:34:48	−69.75	−67.75	4.8C

[a]Origin times and epicenters for 14 earthquakes in Antarctica, 1993–2008, located with the surface-wave detection algorithm. The letter code following the magnitude M indicates the quality of the detection and location: A is the highest quality and C/E is the lowest. Magnitudes are calibrated as described by Ekström (2006).
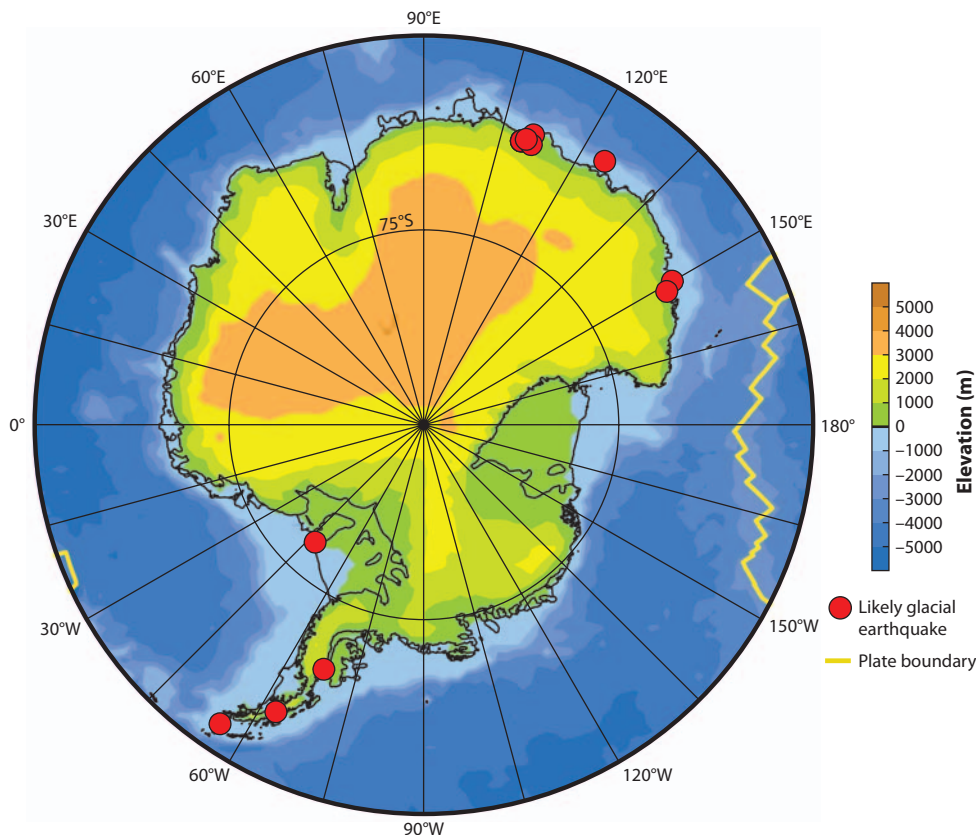
Figure 9

Map of Antarctica showing locations of 14 teleseismic detections that are likely to correspond to glacial earthquakes.

glaciers that generate glacial earthquakes in Greenland have floating tongues no more than a few kilometers long, or no floating tongue at all, such that glacial-earthquake calving events occur near the grounding line. In contrast, most large Antarctic glaciers drain into floating ice shelves or have floating tongues many kilometers long. Calving events of the "silent" type depicted in **Figure 8** may be more likely in this setting, and events that involve capsizing icebergs are likely to occur far from the grounding line, reducing coupling between the applied force and the solid earth.

Several spectacular collapses of floating ice shelves have occurred in Antarctica during the time period included in our detection analysis, including the disintegration of the Larsen A ice shelf in 1995, the Larsen B ice shelf in 2002, and the Wilkins ice shelf in 2008. These collapses included abundant capsizing icebergs, and two of the glacial-earthquake detections reported here (March 18, 2002 and July 21, 2008) may be associated with those events. The small number of earthquakes, in comparison with the ice volume lost, however, suggests that the floating ice shelves may indeed reduce coupling to the solid earth. We note that the Totten and Adams glaciers, located near Casey Station and the Vincennes Bay cluster of earthquake detections, possess relatively short floating tongues.

Few other studies of glacial-earthquake activity in Antarctica are available. Using a surface-wave detection and location algorithm similar to that of Ekström (2006), Chen et al. (2008) reported

the detection of 15 earthquakes occurring in three groups along the Antarctic coastline during the period 1997–2007. The authors speculated that these events were associated with glacial calving or glacial sliding, but they provided no additional information.

Wiens et al. (2008) combined long-period surface-wave observations and GPS measurements of ice displacements to identify a mode of seismogenic stick-slip behavior of the Whillans Ice Stream in West Antarctica. They describe the sudden sliding motion of the ice stream across a basal area of more than 20,000 km^2, with a total displacement of up to 70 cm. The total duration of sliding is observed to be approximately 25 min, and the starting and stopping phases of motion are associated with the radiation of long-period surface waves that are recorded at several hundred kilometers' distance from the ice stream. The stick-slip motion of the ice stream is tidally modulated and occurs regularly twice per day. Little or no slip occurs between the stick-slip events.

Although the spectral characteristics of the Whillans Ice Stream events are similar to the Greenland events, the mechanisms for these two types of glacial earthquakes are distinct. The Whillans Ice Stream earthquakes are slow-sliding events involving large volumes (thousands of cubic kilometers) of ice and small displacements, similar to the physical mechanism initially hypothesized for the Greenland earthquakes (Ekström et al. 2003). The Greenland earthquakes, on the other hand, are associated with glacier calving that involves large displacements of relatively small ($\sim$1 km^3) volumes of ice. The amplitudes of the seismic waves observed by Wiens et al. (2008) are smaller than those radiated by the Greenland events, similar to those expected for an earthquake of $M \sim 3$ rather than one of $M \sim 5$ as in Greenland, despite the large mass involved. One explanation for the relatively weak observed seismic energy may be that the 25-min-long motion of the ice stream does not generate signal in the seismic band, whereas the rapid acceleration that occurs during the starting and stopping phases of the motion generates energy in the seismic band but involves a smaller ice mass.

3.2. Slow Earthquakes in Alaska

In the first paper describing glacial earthquakes, Ekström et al. (2003) identified an earthquake in the Alaska Range on September 4, 1999, as a glacial earthquake based on its anomalous source characteristics and geographical location. The earthquake was shown to have radiated little high-frequency seismic energy, and its long-period surface waves were poorly fit by a moment-tensor earthquake-faulting model but well fit by a single-force landslide model. The earthquake was also found to be located near the Dall glacier, so the authors made a geographical association between the detected phenomenon and the glacier and hypothesized glacier sliding as a plausible mechanism.

Recently, several $M \sim 5$ surface-wave detections in Alaska have been shown to be associated with massive rock avalanches (Ekström et al. 2007, Lipovsky et al. 2008), and the earlier explanation for the 1999 earthquake deserves reexamination. Ekström et al. (2007) found that surface-wave detections for two earthquakes in 2005 and 2007 were associated with rock avalanches at Mount Steller, southern Alaska, and Mount Steele, southern Yukon, respectively, and involved the movement of more than 10^7 m^3 of debris over several kilometers. The low-amplitude, high-frequency seismic radiation from the recent rock avalanches is similar in character to that observed in the 1999 Alaska Range earthquake, as are the long-period surface waves. Following the recent realization that mass-wasting events of the type exemplified by the Mount Steller and Mount Steele events generate globally observable surface waves similar to those caused by glacial earthquakes, a rock-avalanche mechanism for the 1999 earthquake now seems probable to us. However, we are not aware of any independent observations corroborating the occurrence of such an event.

4. OUTSTANDING QUESTIONS

In the six years since the identification of glacial earthquakes by Ekström et al. (2003), rapid progress in understanding the source of the observed seismic waves has been achieved through interdisciplinary efforts employing remote and local data and seismological, geodetic, and glaciological techniques. Important progress has also been achieved in understanding the short-timescale response of outlet glaciers to the earthquake events. Some important questions remain unanswered, and the discoveries of the past six years have generated many new scientific questions.

4.1. Forces Active During Calving and Glacial-Earthquake Seismogenesis

The theoretical work of Tsai et al. (2008) demonstrates that the amplitude of forces acting on the calving face during collapse of large icebergs into the glacial fjord and the timescale during which those forces act are in general agreement with teleseismic observations at periods of 35–150 s. However, we lack a detailed prediction of the time history of these forces and of the forces that might be exerted in the vertical and cross-flow directions. We also lack a good understanding of the way in which the forces exerted by a capsizing iceberg couple into the solid earth. At present, few seismological data are available from near-regional and local distances to assess such models, and teleseismically recorded data do not contain sufficiently high-frequency signals for this analysis because of weak high-frequency excitation at the source and long propagation distances.

The few near-regional recordings that do exist (Amundson et al. 2008, Nettles et al. 2008a, Rial et al. 2009) demonstrate that the seismic signal generated by the ice-loss process as a whole is more complicated than can be explained by a simple view of the capsizing-iceberg mechanism. Amundson et al. (2008, 2010) have suggested a contribution to the glacial-earthquake signal from the interaction of the newly calved iceberg with the fjord bottom, as well as a contribution from ocean loading in the fjord system. Rial et al. (2009) have suggested that some of the signal they observe in the Jakobshavn catchment may be generated upflow from the calving front, possibly also as a result of ice-rock interactions. Seismogenic deformation associated with basal sliding, like that reported in Antarctica (e.g., Anandakrishnan & Bentley 1993, Danesi et al. 2007) and at mountain glaciers (e.g., Walter et al. 2008), may also contribute. Similarly, the stick-slip sliding and associated seismic-wave generation reported by Wiens et al. (2008) is unlikely to be unique to the Whillans Ice Stream and may be occurring undetected in Greenland. With particular combinations of ice parameters, Tsai et al. (2008) were able to produce some models for a glacial-earthquake source involving the loss of basal resistance like that originally invoked by Ekström et al. (2003) and perhaps observed by Wiens et al. (2008). Assessment of any of these possible source mechanisms requires both the collection of high-quality data sets and systematic and careful data analysis. Such analysis has the potential to provide detailed information about the calving process, internal glacier deformation, and ice-bedrock interactions.

4.2. Seasonal and Interannual Variations

The retreat and advance patterns of glacier termini provide a general explanation for the variability in glacial-earthquake frequency on seasonal and interannual timescales. However, many variations in earthquake activity in individual glacier systems remain unexplained. In addition to the difference in timing of the seasonal seismicity peaks at different glaciers noted in Section 2.3.3, individual glaciers appear to respond differently to interannual variations in calving-front position. Whereas the marked increase in glacial-earthquake occurrence at Helheim glacier from 2003 to 2005 (Tsai & Ekström 2007) corresponds with a dramatic retreat of the calving front during the

same time period (Howat et al. 2005, Luckman et al. 2006, Stearns & Hamilton 2007), an equally dramatic—and more rapid—retreat of the calving front at Kangerdlugssuaq glacier (Luckman et al. 2006, Howat et al. 2007, Stearns & Hamilton 2007) in 2005 does not appear to have affected earthquake frequency there.

To explain these variations, better knowledge of the physical controls on calving-front advance and retreat, and on calving style, is required. Although variations in surface melting may affect calving behavior through, for example, its effect on crevasse opening and propagation, it is clear that surface melting does not provide the primary control on calving-front advance or retreat. The seasonal retreat of the calving front at Jakobshavn typically begins in March, well before the start of the melt season; at Kangerdlugssuaq, retreat continues into the winter months, well after the end of the melt season. Sea-ice conditions and variations in water temperature and currents in the fjord system correlate with interannual advance and retreat patterns (e.g., Holland et al. 2008, Howat et al. 2008, Joughin et al. 2008b), but seasonal conditions are poorly known. Some suggestion of atmospheric control is provided by the observation of Joughin et al. (2008a) that the 2006 minimum in glacial-earthquake activity at Helheim glacier coincided with colder-than-average temperatures, and the observation of Moon & Joughin (2008) that calving termini throughout East and Southeast Greenland responded to this temperature low. A better understanding of interactions among ice, ocean, and atmospheric conditions is needed to clarify the mechanisms controlling the timing of large-scale calving events.

4.3. Glacier Response to Glacial-Earthquake Events

Just as limited as our knowledge of glacier-dynamic controls on earthquake occurrence is our understanding of the glacier response to earthquake-generating calving events. Multiple observations (Nettles et al. 2008a,b; Amundson et al. 2008) show that glaciers respond to glacial-earthquake events by abruptly accelerating by several percent. The precise relative timing of the glacial earthquakes and the attendant glacier acceleration remains ambiguous, however, with some indication (Nettles et al. 2008a; see also **Figure 6**) that glacier acceleration may precede long-period seismic-energy release by as much as a few tens of minutes. Resolving this ambiguity would provide insight into the mechanisms by which resistance to glacier flow is lost. Glacier behavior subsequent to such acceleration is not well documented. In at least one case, in which Helheim glacier accelerated by ∼20% near the calving front in response to a double-earthquake event, the velocity increase was sustained throughout the summer season (Nettles et al. 2008a). A series of several such increases could account for the doubling or near-doubling of glacier speed observed at several of Greenland's large outlet glaciers during the past decade (Joughin et al. 2004, Howat et al. 2005, Luckman et al. 2006, Rignot & Kanagaratnam 2006, Stearns 2007). Such an explanation would require that the earthquake-related velocity increases be sustained from one season to the next, and the conditions under which this might occur are currently unknown.

5. CONCLUSIONS

The discovery of glacial earthquakes was serendipitous. The investigation that led to the detection of these earthquakes was motivated by a long-standing question in seismology concerning the existence and nature of slow tectonic earthquakes. The surface-wave detection algorithm was designed to find any seismic source that radiated strong long-period elastic waves, with the anticipation that some tectonic earthquakes with anomalous source characteristics could be found. The detection of $M \sim 5$ earthquakes in Greenland, an area considered essentially aseismic, was a surprise. The circumstances that made the discovery possible were the existence of a high-quality,

global network of seismographs and the archiving of—and open access to—the continuous data from this network. We note that, over the past decade, a number of discoveries of new seismic phenomena have been identified in novel analyses of continuous "noise" signals, such as Earth's hum, episodic tremor in fault zones, subaerial and submarine landslides, iceberg bottom-scraping and bumping, and volcano collapses. Seismological observations can now be used to help elucidate and constrain the physical processes active in these phenomena.

The physical mechanism for glacial earthquakes was initially unknown, and targeted geodetic field experiments were necessary to obtain the observations that have led to the current understanding that the events are directly linked to the calving process. The understanding of glacial earthquakes is thus improving rapidly, although the details of the elastic-wave generation remain unclear. At the same time, the geophysical observations obtained in the field have uncovered new aspects of transient glacier behavior that comprise one expression of the dynamics of glacier deformation. Additional multidisciplinary investigations will be required to advance the understanding of this complex system further.

DISCLOSURE STATEMENT

The authors are not aware of any affiliations, memberships, funding, or financial holdings that might be perceived as affecting the objectivity of this review.

ACKNOWLEDGMENTS

LITERATURE CITED

Amundson JM, Fahnestock M, Truffer M, Brown J, Lüthi MP, Motyka RJ. 2010. Ice mélange dynamics and implications for terminus stability, Jakobshavn Isbræ, Greenland. *J. Geophys. Res.* 115:F01005

Amundson JM, Truffer M, Lüthi MP, Fahnestock M, West M, Motyka RJ. 2008. Glacier, fjord, and seismic response to recent large calving events, Jakobshavn Isbræ, Greenland. *Geophys. Res. Lett.* 35:L22501

Anandakrishnan S, Bentley CR. 1993. Micro-earthquakes beneath Ice Streams B and C, West Antarctica: observations and implications. *J. Glaciol.* 39:455–62

Chen X, Shearer PM, Walker KT, Fricker HA. 2008. Global seismic event detection using surface waves: 15 possible Antarctic glacial sliding events. *Eos Trans. AGU* 89(53), Fall Meet. Suppl., Abstr. C11D-0543

Clarke TS, Echelmeyer K. 1996. Seismic-reflection evidence for a deep subglacial trough beneath Jakobshavn Isbræ, West Greenland. *J. Glaciol.* 42:219–32

Danesi S, Bannister S, Morelli A. 2007. Repeating earthquakes from rupture of an asperity under an Antarctic outlet glacier. *Earth Planet. Sci. Lett.* 253:151–58

Deichmann NJ, Ansorge J, Scherbaum F, Aschwanden A, Bernardi F, Gudmundsson GH. 2000. Evidence for deep icequakes in an Alpine glacier. *Ann. Glaciol.* 31:85–90

de Juan J, Elósegui P, Nettles M, Larsen TB, Davis JL, et al. 2008. Sub-daily glacier flow variations at Helheim Glacier, East Greenland, using GPS. *Eos Trans. AGU* 89(53), Fall Meet. Suppl., Abstr. C31C-0518

Dupont TK, Alley RB. 2005. Assessment of the importance of ice-shelf buttressing to ice-sheet flow. *Geophys. Res. Lett.* 32:L04503

Ekström G. 2006. Global detection and location of seismic sources by using surface waves. *Bull. Seismol. Soc. Am.* 96:1201–12

Ekström G, Hansen RA, Pavlis GL, Lipovsky P. 2007. Seismological detection and analysis of recent landslides in Alaska and the Yukon. *Eos Trans. AGU* 88(52), Fall Meet. Suppl., Abstr. S52B-05

Ekström G, Nettles M. 2002. Detection and location of slow seismic sources using surface waves. *Eos Trans. AGU* 83(47), Fall Meet. Suppl., Abstr. S72E-06

Ekström G, Nettles M, Abers GA. 2003. Glacial earthquakes. *Science* 302:622–24

Ekström G, Nettles M, Tsai VC. 2006. Seasonality and increasing frequency of Greenland glacial earthquakes. *Science* 311:1756–58

Hamilton GS, Khan SA, Schild KM, Stearns LA, Nettles M, et al. 2008. Iceberg calving and flow dynamics at Helheim Glacier, East Greenland, from time-lapse photography. *Eos Trans. AGU* 89(53), Fall Meet. Suppl., Abstr. C13A-0565

Holland DM, Thomas RH, de Young B, Ribergaard MH, Lyberth B. 2008. Acceleration of Jakobshavn Isbræ triggered by warm subsurface ocean waters. *Nat. Geosci.* 1:659–64

Howat IM, Joughin I, Fahnestock M, Smith BE, Scambos TA. 2008. Synchronous retreat and acceleration of southeast Greenland outlet glaciers 2000–06: ice dynamics and coupling to climate. *J. Glaciol.* 54:646–60

Howat IM, Joughin I, Scambos TA. 2007. Rapid changes in ice discharge from Greenland outlet glaciers. *Science* 315:1559–61

Howat IM, Joughin I, Tulaczyk S, Gogineni S. 2005. Rapid retreat and acceleration of Helheim Glacier, east Greenland. *Geophys. Res. Lett.* 32:L22502

Jónsdóttir K, Roberts R, Pohjola V, Lund B, Shomali ZH, et al. 2009. Glacial long period seismic events at Katla volcano, Iceland. *Geophys. Res. Lett.* 36:L11402

Joughin I, Abdalati W, Fahnestock M. 2004. Large fluctuations in speed on Greenland's Jakobshavn Isbræ glacier. *Nature* 432:608–10

Joughin I, Howat I, Alley RB, Ekström G, Fahnestock M, et al. 2008a. Ice-front variation and tidewater behavior on Helheim and Kangerdlugssuaq Glaciers, Greenland. *J. Geophys. Res.* 113:F01004

Joughin I, Howat IM, Fahnestock M, Smith B, Krabill W, et al. 2008b. Continued evolution of Jakobshavn Isbræ following its rapid speedup. *J. Geophys. Res.* 113:F04006

Kawakatsu H. 1989. Centroid single force inversion of seismic waves generated by landslides. *J. Geophys. Res.* 94(B9):12363–74

Lipovsky PS, Evans SG, Clague JJ, Hopkinson C, Couture R, et al. 2008. The July 2007 rock and ice avalanches at Mount Steele, St. Elias Mountains, Yukon, Canada. *Landslides* 5:445–55

Luckman A, Murray T, de Lange R, Hanna E. 2006. Rapid and synchronous ice-dynamic changes in East Greenland. *Geophys. Res. Lett.* 33:L03503

Moon T, Joughin I. 2008. Changes in ice front position on Greenland's outlet glaciers from 1992 to 2007. *J. Geophys. Res.* 113:F02022

Nettles M, Ahlstrøm A, Elósegui P, Hamilton G, Khan S, et al. 2006. Helheim 2006: Integrated geophysical observations of glacier flow. *Eos Trans. AGU* 87(52), Fall Meet. Suppl., Abstr. S44A-08

Nettles M, Larsen TB, Elósegui P, Hamilton GS, Stearns LA, et al. 2008a. Step-wise changes in glacier flow speed coincide with calving and glacial earthquakes at Helheim Glacier, Greenland. *Geophys. Res. Lett.* 35:L24503

Nettles M, Larsen TB, Elósegui P, Hamilton GS, Stearns LA, et al. 2008b. Glacier acceleration, glacial earthquakes, and ice loss at Helheim Glacier, Greenland. *Eos Trans. AGU* 89(53), Fall Meet. Suppl., Abstr. G23A-02

Nick FM, Vieli A, Howat IM, Joughin I. 2009. Large-scale changes in Greenland outlet glacier dynamics triggered at the terminus. *Nat. Geosci.* 2:110–14

O'Neel S, Marshall HP, McNamara DE, Pfeffer WT. 2007. Seismic detection and analysis of icequakes at Columbia Glacier, Alaska. *J. Geophys. Res.* 112:F03S23

Paterson, WSB. 1994. *The Physics of Glaciers*. New York: Butterworth Heinemann. 481 pp. 3rd ed.

Qamar A. 1988. Calving icebergs: a source of low-frequency seismic signals from Columbia Glacier, Alaska. *J. Geophys. Res.* 93(B6):6615–23

Rial JA, Tang C, Steffen K. 2009. Glacial rumblings from Jakobshavn ice stream, Greenland. *J. Glaciol.* 55:389–99

Rignot E, Kanagaratnam P. 2006. Changes in the velocity structure of the Greenland ice sheet. *Science* 311:986–90

Stearns LA. 2007. *Outlet glacier dynamics in East Greenland and East Antarctica*. Ph.D. thesis. Univ. Maine, Orono. 113 pp.

Stearns LA, Hamilton GS. 2007. Rapid volume loss from two East Greenland outlet glaciers quantified using repeat stereo satellite imagery. *Geophys. Res. Lett.* 34:L05503

Steffen K, Nghiem SV, Huff R, Neumann G. 2004. The melt anomaly of 2002 on the Greenland Ice Sheet from active and passive microwave satellite observations. *Geophys. Res. Lett.* 31:L20402

Stuart G, Murray T, Brisbourne A, Styles P, Toon S. 2005. Seismic emissions from a surging glacier: Bakaninbreen, Svalbard. *Ann. Glaciol.* 42:151–57

Tsai VC, Ekström G. 2007. Analysis of glacial earthquakes. *J. Geophys. Res.* 112:F03S22

Tsai VC, Rice JR, Fahnestock M. 2008. Possible mechanisms for glacial earthquakes. *J. Geophys. Res.* 113:F03014

Walter F, Deichmann N, Funk M. 2008. Basal icequakes during changing subglacial water pressures beneath Gornergletscher, Switzerland. *J. Glaciol.* 54:511–21

Weaver CS, Malone SD. 1979. Seismic evidence for discrete glacier motion at the rock-ice interface. *J. Glaciol.* 23:171–84

Wiens DA, Anandakrishnan S, Winberry JP, King MA. 2008. Simultaneous teleseismic and geodetic observations of the stick-slip motion of an Antarctic ice stream. *Nature* 453:770–74

Wolf LW, Davies JN. 1986. Glacier-generated earthquakes from Prince William Sound, Alaska. *Bull. Seismol. Soc. Am.* 76:367–79

Zwally HJ, Abdalati W, Herring T, Larson K, Saba J, Steffen K. 2002. Surface melt-induced acceleration of Greenland ice-sheet flow. *Science* 297:218–22

**Annual Review
of Earth and
Planetary Sciences**

Volume 38, 2010

Contents

Indexes

Errata

An online log of corrections to *Annual Review of Earth and Planetary Sciences* articles
may be found at http://earth.annualreviews.org

ANNUAL REVIEWS

It's about time. Your time. It's time well spent.

New From Annual Reviews:

Annual Review of Statistics and Its Application

Volume 1 • Online January 2014 • http://statistics.annualreviews.org

Editor: **Stephen E. Fienberg,** *Carnegie Mellon University*

Associate Editors: **Nancy Reid,** *University of Toronto*

Stephen M. Stigler, *University of Chicago*

The *Annual Review of Statistics and Its Application* aims to inform statisticians and quantitative methodologists, as well as all scientists and users of statistics about major methodological advances and the computational tools that allow for their implementation. It will include developments in the field of statistics, including theoretical statistical underpinnings of new methodology, as well as developments in specific application domains such as biostatistics and bioinformatics, economics, machine learning, psychology, sociology, and aspects of the physical sciences.

Complimentary online access to the first volume will be available until January 2015.

Access this and all other Annual Reviews journals via your institution at **www.annualreviews.org**.